Lateral Spatial Effects of Feedback in Gain-Guided and Broad-Area Semiconductor Lasers

John R. Marciante and Govind P. Agrawal, *Fellow, IEEE*

***Abstract*—Starting from Fresnel diffraction theory, we derive analytic expressions for the lateral spatial dependence of feedback fields for the cases of conventional and phase-conjugate optical feedback. By using numerical simulations we show that for narrow-stripe gain-guided lasers, both types of optical feedback from an external cavity can convert the twin-lobed far fields into a nearly single-lobed far field. We also find that conventional and phase-conjugate feedbacks in broad-area lasers induce a spatial modulation of the lateral field that increases the tendency for filamentation at moderate (−30 dB) feedback levels.**

I. Introduction

OPTICAL feedback is often a practical problem for most applications of semiconductor lasers. For example, in fiber-optic applications, the laser light is focused onto an optical fiber. At the fiber–air interface, some light gets reflected back to the laser. Similarly, in optical data recording, the laser light is focused onto a rotating disk, which reflects the light, some of which gets back into the laser. Conventional optical feedback (COF), produced by reflecting surfaces, has many detrimental effects that have been extensively studied. At low levels, feedback can induce linewidth broadening or narrowing [1], depending on wavelength-size variations in the external-cavity length. At higher levels, the laser undergoes coherence collapse [2]–[4], entering a chaotic regime where the laser linewidth can be as large as as 50 GHz. Multimode models have shown mode-hopping and chaos [5], and methods of controlling these detrimental effects have been considered [5]–[6]. Studies have also been done for modeling the effects of phase-conjugate feedback (PCF) on single-mode semiconductor lasers [7]–[10]. The results have shown regions of stability [8] and reduced noise [9], as well as regions of chaotic behavior [10]. However, until a recent experiment [11], all previous work on feedback in semiconductor lasers has concentrated on narrow-stripe devices, and thus no attention has been given to the spatial mode of the laser.

The experiment of Bossert *et al.* [11] showed that optical feedback can severely alter the lateral mode characteristics in a wide-stripe laser. In this study, they used broad-area tapered semiconductor lasers [12], [13] with gain regions that flared to a 200–300-μm-wide lateral output. The flared region helps to maintain the integrity of the lateral mode by allowing it to expand as the optical beam propagates through the gain region, resulting in a high-power, diffraction-limited output. Under COF, the study showed severe degradation of the far-field image with a significantly reduced power in the central lobe.

In order to understand the observed behavior more clearly, we need an accurate model that can predict the spatial effects of feedback. In this paper, we use Fresnel diffraction theory to derive an expression for the optical field that is reflected back into the laser cavity. We then apply this result to a computer model that solves for the lateral mode evolution accurately by using a split-step Fourier (beam-propagation) method. The numerical model is used to study the effects of conventional and phase-conjugate feedback on narrow-stripe as well as broad-area semiconductor lasers.

II. Feedback Model

First, let us phenomenologically consider what happens to the lateral mode in the external cavity. Fig. 1 depicts he propagation of the lateral field in the feedback cavity with the return trip longitudinally "unfolded" to the other side of the mirror. Since most lens combinations can be analytically combined to form a single compound lens, we consider only one lens in the external cavity. It is well known that the lateral mode of gain-guided lasers exhibits a strong astigmatic character at the output facet [14]. In Fig. 1, we represent this divergent wavefront and include an additional phase aberration to allow us to track its lateral transformation through the system. The purpose of the lens is to focus the diverging wavefront at the mirror. In most practical applications, the focused spot is likely to be as small as possible to maximize the coupling to the target. This spot will not be an image of the near field, but rather an image of the virtual source [11], a point within the laser from which the light appears to be originating. Upon reflection at the mirror, the wavefront flips laterally about the optic axis, and begins its journey back to the laser. On its arrival, the wavefront is converging at the facet with the lateral axis inverted, and the phase aberration still ahead of the rest of the wavefront (see Fig. 1).

In the case of PCF, the mirror in Fig. 1 is replaced by a phase-conjugate mirror. Tracking the transformation of the PCF, we find that since phase-conjugated fields exhibit wavefront reversal (as indicated in Fig. 1), the returning wavefront is converging at the facet with the lateral axis unchanged, but the phase aberration is now behind the wavefront.

For implementing the effects of feedback accurately, we should generally consider wave propagation in both the lateral dimension x and the transverse dimension y (out of the plane

Manuscript received March 11, 1996; revised May 24, 1996.

J. R. Marciante is with the The Institute of Optics, University of Rochester, Rochester, NY 14627 USA. He is also with the Semiconductor Laser Branch, USAF Phillips Laboratory, Kirtland AFB, NM 87117-5776 USA.

G. P. Agrawal is with the The Institute of Optics, University of Rochester, Rochester, NY 14627 USA.

Publisher Item Identifier S 0018-9197(96)06408-1.

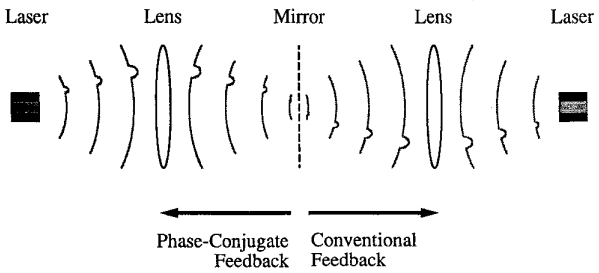

Fig. 1. Schematic illustration of the wavefront propagation in the external cavity for the case of conventional and phase-conjugate optical feedback. The return trip is "unfolded" for clarity in the case of conventional feedback.

of the paper in Fig. 1). However, since the transverse field has a symmetric profile with negligible curvature due to index guiding inside the laser, axial inversion has no effect on it. For this reason, it is justified to deal with the lateral field only by using standard Fresnel diffraction theory [15], [16]. If the field at the facet is given by $E_1(x)$, we can calculate the field $E_2(x')$ at the lens by using the integral

$$E_2(x') = i\frac{\exp(ik_0L_1)}{\sqrt{\lambda L_1}}\int_{-\infty}^{\infty} dx E_1(x)\exp\left[\frac{i\pi}{\lambda L_1}(x-x')^2\right] \tag{1}$$

where $\lambda = 2\pi/k_0$ is the optical wavelength and L_1 is the distance between the laser facet and the lens. The lens of focal length F imparts a quadratic phase upon the impinging wavefront, so the field just after the lens $E_2^+(x')$ is given by

$$E_2^+(x') = E_2(x')\exp\left(-\frac{i\pi}{\lambda F}x'^2\right). \tag{2}$$

Further propagation to the mirror results in an equation similar to (1), with the field at the mirror, $E_3(x'')$, given by

$$E_3(x'') = i\frac{\exp(ik_0L_2)}{\sqrt{\lambda L_2}}\int_{-\infty}^{\infty} dx' E_2^+(x') \cdot \exp\left[\frac{i\pi}{\lambda L_2}(x'-x'')^2\right] \tag{3}$$

where L_2 is the distance between the lens and the mirror. By substituting (1) and (2) into (3), we can perform the integral over x'. By setting $L_1 = F$ as is commonly done in experiments (for beam collimation), we obtain

$$E_3(x'') = -\frac{\exp(ik_0L_{\text{ext}})}{\sqrt{\lambda F}}\int_{-\infty}^{\infty} dx[E_1(x)\exp(-i\beta x^2)] \cdot \exp\left(-\frac{i2\pi}{\lambda F}x''x\right) \tag{4}$$

where $\beta = (\pi/\lambda F)(L_2/F-1)$ and $L_{\text{ext}} = L_1+L_2$ is the total external cavity length. Note that if we make $\beta = 0$ by choosing $L_2 = F$, we have the actual far field represented at the mirror [the Fourier transform of the laser output $E_1(x)$]. For an index guided-laser, this would be the smallest spot attainable. However, as discussed previously, gain-guided lasers exhibit a curved wavefront. To attain the smallest spot on the intended target for these devices, the image is focused to remove the astigmatic curvature from the near field. Thus, one must choose the distance L_2 such that the lens-induced curvature β cancels the astigmatic quadratic curvature of the wavefront at the laser output facet. Since the condition $L_1 = F$ indicates that the flat transverse mode profile will be collimated, the lens will re-image this profile upon itself in exact duplication, thus justifying our neglect of feedback transformation for the transverse mode.

To obtain the feedback wavefront, we need to repeat this calculation in reverse. The details are similar to the previous calculation of $E_3(x'')$, and the resultant feedback wavefront $E_{FB}(x)$ is given by

$$E_{FB}(x) = -\frac{\exp(ik_0L_{\text{ext}})}{\sqrt{\lambda F}}\exp(-i\beta x^2)\int_{-\infty}^{\infty} dx'' E_3^+(x'') \cdot \exp\left(-\frac{i2\pi}{\lambda F}xx''\right) \tag{5}$$

where $E_3^+(x'')$ is the field just after reflection from the mirror. The form of (5) is identical to that of (4), except that the quadratic phase component is outside the integral. Thus, the reflected field is Fourier transformed with a convergent phase factor added.

For the case of COF, the effect of the mirror is to reverse the direction of propagation with a reduced amplitude, so the field just after reflection is $E_3^+(x'') = \sqrt{R_{FB}}E_3(x'')$, where R_{FB} is the mirror reflectivity. By using (4) and (5), we obtain the following simple expression for the feedback field

$$E_{\text{COF}}(x) = \sqrt{R_{FB}}\exp(i2k_0L_{\text{ext}})[\exp(-i2\beta x^2)E_1(-x)]. \tag{6}$$

As expected from Fig. 1, the feedback field has its curvature inverted and its lateral axis flipped. From a practical point of view, one might consider the case where the transverse mode is focused to a minimal spot on the target as well. Since the transverse and lateral directions appear to have virtual sources at different points (due to the different wavefront curvatures), one must use cylindrical lenses to affect the foci of these sources independently. In our theory, this implies a different set of F, L_1, and L_2 for the transverse direction. The analysis is the same, however, with identical results.

In the case of PCF, the field after the phase-conjugate mirror can be written as $E_3^+(x'') = \sqrt{R_{FB}}\exp(i\phi_{\text{PCM}})E_3^*(x'')$ where R_{FB} is the reflectivity of the phase-conjugate mirror, and a constant phase ϕ_{PCM} has been added to account for any phase shift occuring at the mirror. By using (4) and (5), we obtain the following expression for the PCF field

$$E_{\text{PCF}}(x) = \sqrt{R_{FB}}\exp(i\phi_{\text{PCM}})E_1^*(x). \tag{7}$$

Again, this result proves our intuition to be correct. The field returning to the laser is simply the phase-conjugate of the field that left, with no accumulated phase over the external-cavity length.

What effect will these feedback fields have when they return into the laser? If we recall that the intracavity field at the laser facet has a diverging phasefront, in the case of COF, this diverging wavefront combines coherently with a convergent fed-back wavefront with phase aberrations inverted about the lateral axis. By contrast, in the PCF case the two

wavefronts would recombine in such a way as to cancel the phase aberrations.

III. Semiconductor Laser Model

To use the results of Section II, we first need to model the evolution of the lateral mode in the laser cavity itself. We consider a semiconductor laser operating continuously at a constant current density, and solve the intracavity forward and backward propagating waves iteratively while including diffraction, carrier diffusion, and spatial hole burning. Since we are looking to solve for the lateral distribution (along the x axis) of the intracavity field, we decompose the electric field in terms of counterpropagating waves using Maxwell's equations and obtain a set of two coupled paraxial wave equations:

$$\pm\frac{\partial E_m}{\partial z} = \frac{i}{2k}\frac{\partial^2 E_m}{\partial x^2} + \left[\frac{1}{2}\Gamma(1-i\alpha)g(N) - \frac{\alpha_{\text{int}}}{2}\right]E_m \quad (8)$$

where the $+$ or $-$ sign is chosen for the forward ($m = f$) and backward ($m = b$) traveling waves respectively, $k = n_{\text{eff}}k_0$ is the mode propagation constant with n_{eff} being the effective index of refraction, Γ is the transverse confinement factor, α is the linewidth-enhancement factor, α_{int} is internal loss, and $g(N)$ is the local carrier-dependent gain assumed to be of the form $g(N) = a(N - N_0)$. Here, a is the gain cross section and N_0 is the transparency value for the carrier density ($g = 0$ at $N = N_0$). The carrier density distribution can be accounted for by solving the diffusion equation [17]

$$D\frac{\partial^2 N}{\partial x^2} = -\frac{J(x)}{qd} + \frac{N}{\tau_{nr}} + BN^2 + \frac{\Gamma g(N)}{\hbar\omega}(|E_f|^2 + |E_b|^2) \quad (9)$$

where D is the diffusion constant, $J(x)$ is the injected current density, q is the magnitude of the electron charge, d is the active-layer thickness, τ_{nr} is the nonradiative lifetime, and B is the spontaneous-emission coefficient. For uniform injection over the stripe width w, $J(x) = J_0$ for $|x| < w/2$, and 0, otherwise.

To investigate the effects of feedback, we have solved (8) and (9) numerically by using a split-step Fourier or beam-propagation method iteratively [17], [18]. We incorporate feedback into the boundary conditions in the following form:

$$E_f(x,0) = \sqrt{R_0}E_b(x,0) \quad (10a)$$

$$E_b(x,L) = \sqrt{R_L}E_f(x,L) + \sqrt{f_{\text{ext}}}E_{FB}(x,L). \quad (10b)$$

The facets are located at $z = 0$ and $z = L$, with R_0 and R_L being their respective reflectivities. The external feedback fraction $f_{\text{ext}} = \eta R_{FB}(1 - R_L)^2$ contains the coupling efficiency η and the feedback mirror reflectivity R_{FB}. The term E_{FB} represents the feedback field which can be either E_{COF} or E_{PCF} as defined in (6) and (7), respectively. For a given laser, the quadratic curvature β is calculated from the simulated mode profile of the solitary laser (i.e., no feedback).

While both COF and PCF initially yield fields with inverted curvatures [(6) and (7)], it is significant to note the differences upon iteration. As noted in Section II, the feedback and reflected intracavity fields coherently add to flatten the mode wavefront. As the field returns to the facet one round-trip later, its corresponding COF field will have a more convergent wavefront due to the flattened mode wavefront and constant value of β. Thus, as the mode flattens within the laser cavity, the COF field becomes more highly convergent upon the facet. In the case of PCF, since the fed-back field does not depend on β, but rather on the conjugate of the intracavity field, then as the wavefront of the laser mode flattens, the PCF field flattens as well to cancel exactly the mode wavefront curvature. Thus, as the mode flattens within the laser cavity, the PCF field flattens accordingly.

TABLE I
Parameter Values Used in Numerical Simulations

Physical quantity	Symbol	Value
Cavity length	L	250 μm
Contact stripe width	w	5 μm, 50 μm
Active-layer thickness	d	200 nm
Transverse confinement factor	Γ	0.2
Facet power reflectivities	R_0, R_L	0.35
Laser wavelength	λ	820 nm
Effective index	n_{eff}	3.5
Linewidth-enhancement factor	α	3
Internal loss	α_{int}	10 cm^{-1}
Gain cross-section	a	1.5 x 10^{-16} cm^2
Diffusion constant	D	33 cm^2/s
Transparency carrier density	N_0	1.0 x 10^{18} cm^{-3}
Non-radiative lifetime	τ_{nr}	5 ns
Spontaneous-emission coefficient	B	1.4 x 10^{-10} cm^3/s

The iteration procedure is initialized by assuming a super-Gaussian profile for the lateral mode. The lateral mode profile changes initially during multiple round-trips inside the laser cavity and settles down to a fixed shape after 15–20 round-trips if a stable lateral mode exists for a given set of operating parameters. If the lateral mode does not stabilize even after 100 round-trips, the laser is quantified as "unstable" for that set of operating parameters. Table I shows the parameter values used for numerical simulations. These values are appropriate for a stripe-geometry AlGaAs semiconductor laser operating near 820 nm.

IV. Gain-Guided Laser Simulations

We start by simulating a laser with a 5-μm wide stripe contact operating nearly twice above threshold. Fig. 2(a) and (b) show the near- and far-field lateral profiles for the solitary laser (no feedback). The far field clearly shows the "rabbit ears" that are characteristic of narrow-stripe gain-guided semiconductor lasers, a feature that is attributed to the astigmatic curvature of the near-field [14]. We introduce feedback such that the center of the wavefront is in phase with the reflected wavefront [i.e., $2k_0L_{\text{ext}} = 2m\pi$, where m is an arbitrary integer, in (6)]. Fig. 2(c) and (d) show the near- and far-field profiles for the case of relatively weak feedback (−22.3 dB). As the feedback is increased, the two peaks seen in the far-field structure of Fig. 2(b) begin to move closer. The physical mechanism for this phenomenon is the interference of the two wavefronts, one reflected at the laser facet and the other reflected at the

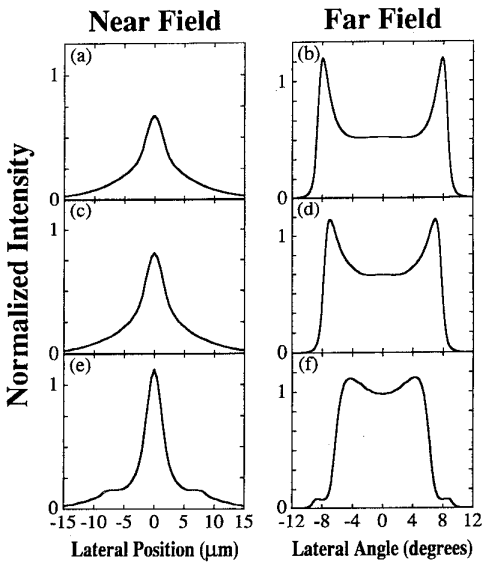

Fig. 2. Near-field (left column) and far-field (right column) profiles for a 5-μm stripe-width laser with in-phase conventional feedback. Feedback power levels are $f_{\text{ext}} = 0$ (top row), -22.3 dB (middle row), and -12.3 dB (bottom row). A normalized vertical scale is used for both near and far fields.

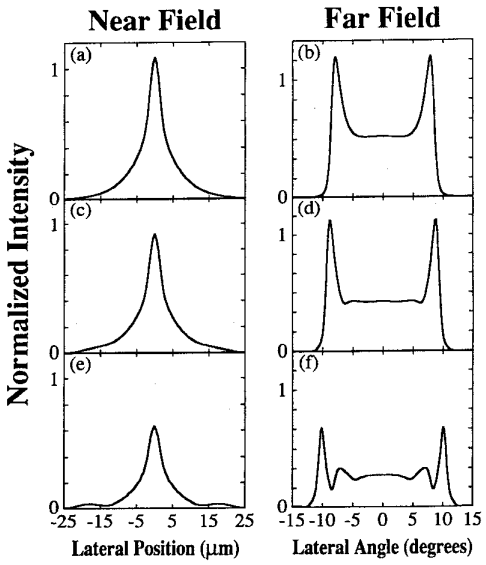

Fig. 3. Same as in Fig. 2 except with out-of-phase conventional feedback.

external cavity mirror. As discussed earlier, these wavefronts have opposite curvatures, resulting in a milder curvature of the net reflected field. This interference is clearly seen in Fig. 2(e) for a feedback level of -12.3 dB, where the near-field peak is narrower and more intense due to constructive interference. However, since the wavefront is curved, the two reflected fields become out of phase as the lateral distance from the peak increases. This destructive interference is also seen in Fig. 2(e) where the wings of the near field are suppressed and exhibit a fringe-like structure. At the same time, the result of this interference is to produce a nearly single-lobed far field, as displayed in Fig. 2(f). One may want to increase the feedback further in an attempt to create a more Gaussian-like profile in the far field. However, if the wavefront becomes too flat, the gain-guided structure cannot support it. For our simulations, this results in an unstable laser profile, occurring at feedback levels exceeding -12 dB.

If we choose the two interfering fields to be out of phase at the wavefront center ($x = 0$) instead of being in phase, then the lateral mode curvature increases instead with feedback. This leads to a broadening of the laser mode, and subsequently a spreading of the peaks in the far field, as seen in Fig. 3. In Fig 3(e), we can clearly see the impact of destructive interference occurring at the center of the near field together with an oscillatory structure in the wings. The increased curvature also results in additional lobes appearing in the far field, as displayed in Fig. 3(d) and 3(f). Similar to the in-phase case, the wavefront can eventually become too curved for the gain-guided structure to support it, resulting in an unstable laser profile.

The effects of PCF are similar to the results obtained with in-phase conventional feedback, as shown in Fig. 4. As discussed in Section III, the nature of the PCF is different than that of COF in that it provides a flattened curvature

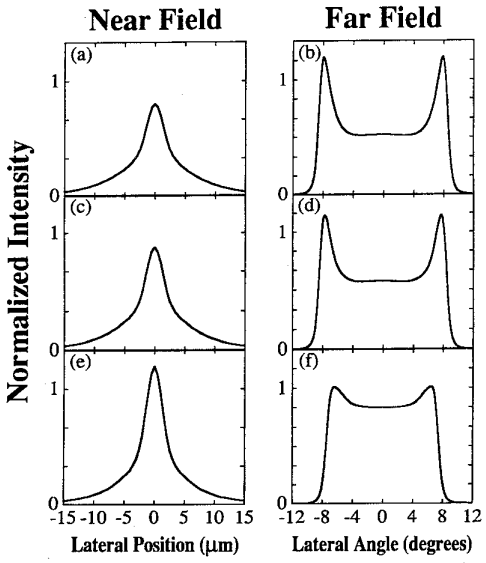

Fig. 4. Same as in Fig. 2 except with phase-conjugate feedback. Feedback power levels are $f_{\text{ext}} = 0$ (top row), -28.3 dB (middle row), and -18.3 dB (bottom row).

on successive round-trip iterations. This produces an in-phase feedback situation which leads to some differences between Figs. 2 and 4. The main qualitative difference is the absence of any fringe-like oscillatory structure in the case of PCF, as noted by comparing Figs. 2(e) and 4(e). This feature can be explained by noting that the phase-conjugate case leads to a situation where there is in-phase overlap over most of the wavefront between the feedback field and the field reflected at the facet. Another difference from the in-phase COF results is that lower levels of PCF are needed to produce the same effects: the nearly single-lobed far field in Fig. 4(f) is obtained at a feedback level of -18.3 dB. In fact, the mode becomes unstable at levels larger than -18 dB.

Similar simulations were performed for an index guided structure of the same stripe width. The results showed an immunity of the lateral profile to spatial effects of feedback. This result is due to the waveguiding produced as a result of the index step: the mode is predetermined by the waveguide structure and exhibits a flat phase profile in the lateral direction. Thus, the inverted feedback wavefront is still planar and no spatial effects can be induced.

V. Broad-Area Laser Simulations

In this section, we study the feedback effects in broad-area semiconductor lasers. Stripe-geometry broad-area lasers exhibit a lateral-mode instability, known as filamentation and caused by the carrier-induced index changes governed by the linewidth-enhancement factor α [19]. We have seen that the feedback can significantly alter the lateral mode by reducing mode curvature, and either symmetrizing (conventional feedback) or removing (phase-conjugate feedback) other phase aberrations. Since filamentation occurs due to a phase-related phenomenon known as self-focusing, it is reasonable to assume that these feedback effects may have some beneficial effect on reducing filamentation tendencies. In fact, it has been demonstrated that the use of phase conjugation can avoid filamentation in a double-pass amplifier configuration [20]. Using the same laser described earlier and increasing the stripe width to 50 μm, we were not able to find any set of parameters where filamentation was avoided.

In order to investigate the effects of feedback on the lateral mode without the presence of filamentation, we set $\alpha = 0$. Fig. 5(a) shows the resulting near-field profile in the absence of feedback with "bat ears" near the edge of the current stripe. This shape is due to effects at the lateral edges of the gain region and is typical of structures that use different geometries to avoid filamentation [21]. Fig. 5(b)–(e) shows that if we add either conventional or phase-conjugate feedback, the near-field becomes deeply modulated laterally, having the appearance of "steady-state" filaments. For the COF case, the modulation is caused by the interference of the wavefronts. Since the mode is so wide, the opposing wavefronts will oscillate between being in and out of phase as the lateral distance from the mode center increases, similar to the cases shown in Figs. 2 and 3. For the PCF case, the mode is altered but the general structure remains intact since the effect of the PCF is to flatten the wavefront without interference effects, as discussed in Section IV. It has been observed that in semiconductor lasers in which the geometry and operating conditions are such that filamentation does not occur under cw operation, a modulation of the lateral field can lead to filamentation [22]–[24]. Certainly, the added modulation resulting from feedback will only complicate the filamentation problem. Indeed, in the case of feedback in tapered-stripe broad-area lasers [11], the device showed evidence of filamentation [25] in the presence of feedback even when the geometry of the laser was chosen to avoid the filamentation problem. By adding an axial variation to the current contact, we could simulate the tapered-stripe laser used in the experiment of [11]. Our results showed that although such a stripe avoids

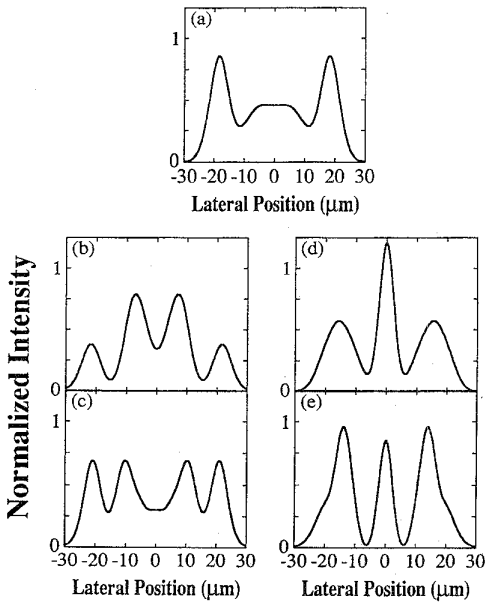

Fig. 5. Near-field profiles for a 50-μm stripe-width laser with $\alpha = 0$ (a) no feedback; (b) −28.3-dB conventional feedback power; (c) −21.3-dB conventional feedback power; (d) −28.3-dB phase-conjugate feedback power; (e) −18.3-dB phase-conjugate feedback power. A normalized vertical scale is used.

the problem of filamentation for the solitary laser, the mode profile becomes unstable under feedback. For our CW analysis, this unstable result implies a dynamic lateral instability that leads to filamentation [19]. A recent experimental study [26] of lateral feedback dynamics in these tapered gain regions has also shown the dynamic instability of the lateral mode.

VI. Conclusion

We have derived analytic expressions for the lateral dependence of feedback fields for both the cases of conventional and phase-conjugate feedback that need to be implemented in any realistic simulation of feedback effects in broad-area semiconductor lasers. By using optical feedback in an external cavity, we can narrow the lateral mode and simultaneously produce a nearly single-lobed far field for narrow-stripe gain-guided lasers, thereby improving the device. We have shown evidence that in broad-area lasers, conventional and phase-conjugate feedbacks induce a modulation of the lateral field that increases the tendency for filamentation at moderate (−30 dB) feedback levels. Finally, we have seen evidence of the dynamic filamentation instability found experimentally in tapered-gain devices under optical feedback.

Acknowledgment

The authors wish to thank D. J. Bossert for a critical reading of the manuscript.

References

[1] G. P. Agrawal, "Line narrowing in a single-mode injection laser due to external optical feedback," *IEEE J. Quantum Electron.*, vol. 20, pp. 468–471, 1984.

[2] G. C. Dente, P. S. Durkin, K. A. Wilson, C. E. Moeller, "Chaos in the coherence collapse of semiconductor lasers," *IEEE J. Quantum Electron.*, vol. 24, pp. 2441–2447, 1988.

[3] S. L. Woodward, T. L. Koch, and U. Koren, "The onset of coherence collapse in DBR lasers," *IEEE Photon. Technol. Lett.*, vol. 2, pp. 391–394, 1990.
[4] G. H. M. van Tartwijk and D. Lenstra, "Semiconductor lasers with optical injection and feedback," *J. Eur. Opt. Soc. B: Quantum Semiclass. Opt.*, vol. 7, pp. 83–143, 1995, and references therein.
[5] A. T. Ryan, G. P. Agrawal, G. R. Gray, and E. C. Cage, "Optical-feedback-induced chaos and its control in multimode semiconductor lasers," *IEEE J. Quantum Electron.*, vol. 30, pp. 688–679, 1994.
[6] G. R. Gray, A. T. Ryan, G. P. Agrawal, and E. C. Cage, "Control of optical-feedback-induced laser intensity noise in optical data recording," *Opt. Eng.*, vol. 32, pp. 739–745, 1993.
[7] G. P. Agrawal and J. T. Klaus, "Effect of phase-conjugate feedback on semiconductor laser dynamics," *Opt. Lett.*, vol. 16, pp. 1325–1327, 1991.
[8] G. H. M. van Tartwijk, H. J. C. van dar Linden, and D. Lenstra, "Theory of a diode laser with phase-conjugate feedback," *Opt. Lett.*, vol. 17, pp. 1590–1592, 1992.
[9] G. P. Agrawal and G. R. Gray, "Effect of phase-conjugate feedback on the noise characteristics of semiconductor lasers," *Phys. Rev. A*, vol. 46, pp. 5890–5898, 1992.
[10] G. R. Gray, D. Huang, and G. P. Agrawal, "Chaotic dynamics of semiconductor lasers with phase-conjugate feedback," *Phys. Rev. A*, vol. 49, pp. 2096–2105, 1994.
[11] D. J. Bossert, J. R. Marciante, and M. W. Wright, "Feedback effects in tapered broad area semiconductor lasers and amplifiers," *IEEE Photon. Technol. Lett.*, vol. 7, pp. 470–472, 1995.
[12] S. O'Brien, D. Welch, R. Parke, D. Mehuys, K. Dzurko, R. J. Lang, R. Waarts, and D. Scrifes, "Operating characteristics of a high-power monolithically integrated flared amplifier master oscillator power amplifier," *IEEE J. Quantum Electron.*, vol. 29, pp. 2052–2057, 1993.
[13] E. S. Kintzer, J. N. Walpole, S. R. Chinn, C. A. Wang, and L. J. Missaggia, "High-power strained-layer amplifiers and lasers with tapered gain regions," *IEEE Photon. Technol. Lett.*, vol. 5, pp. 605–608, 1993.
[14] G. P. Agrawal and N, K, Dutta, *Semiconductor Lasers*, 2nd ed. New York: Van Nostrand Reinhold, 1993.
[15] J. W. Goodman, *Introduction to Fourier Optics*. New York: McGraw-Hill, 1968.
[16] J. D. Gaskill, *Linear Systems, Fourier Transforms, and Optics*. New York: Wiley, 1978.
[17] G. P. Agrawal, "Fast-Fourier-transform based beam-propagation model for stripe-geometry semiconductor lasers: inclusion of axial effects," *J. Appl. Phys.*, vol. 56, pp. 3100–3109, 1984.
[18] G. C. Dente and M. L. Tilton, "Modeling broad-area semiconductor optical amplifiers," *IEEE J. Quantum Electron.*, vol. 20, pp. 76–88, 1993.
[19] J. R. Marciante and G. P. Agrawal, "Nonlinear mechanisms of filamentation in broad-area semiconductor lasers," *IEEE J. Quantum Electron.*, vol. 32, pp. 590–596, Apr. 1996.
[20] W. W. Chow and D. Depatie, "Wave-optical effects in semiconductor laser amplifiers," *J. Appl. Phys.*, vol. 65, pp. 4124–4132, 1989.
[21] D. Mehuys, S. O'Brien, R. J. Lang, A. Hardy, and D. F. Welch, "5W, diffraction-limited, tapered-stripe unstable resonator semiconductor laser," *Electron. Lett.*, vol. 30, pp. 1855–1856, 1994.
[22] A. H. Paxton and G. C. Dente, "Filament formation in semiconductor laser gain regions," *J. Appl. Phys.*, vol. 70, pp. 1–6, 1991.
[23] R. J. Lang, D. Mehuys, A. Hardy, K. M. Dzurko, and D. F. Welch, "Spatial evolution of filaments in broad area diode laser amplifiers," *Appl. Phys. Lett.*, vol. 62, pp. 1209–1211, 1993.
[24] L. Goldberg, M. R. Surette, and D. Mehuys, "Filament formation in a tapered GaAlAs optical amplifier," *Appl. Phys. Lett.*, vol. 62, pp. 2304–2306, 1993.
[25] M. Tamburrini, L. Goldberg, and D. Mehuys, "Periodic filaments in reflective broad area semiconductor optical amplifiers," *Appl. Phys. Lett.*, vol. 60, pp. 1292–1294, 1992.
[26] M. W. Wright, D. J. Bossert, and G. C. Dente, "Temporal dynamics and filamentation in tapered broad area semiconductor lasers with feedback," in *OSA Annu. Meet. Dig.*, Washington, DC: Opt. Soc. Amer., Sept. 1995, paper FK9.

John R. Marciante, for photograph and biography, see p. 596 of the April issue of this JOURNAL.

Govind P. Agrawal (M'83–SM'86–F'96), for photograph and biography, see p. 596 of the April issue of this JOURNAL.